UNIVERSITY OF CALIFORNIA,
IRVINE

Mathematical Modeling of T-cell Exhaustion and PD-1 Blockade in Chronic Infections

THESIS

submitted in partial satisfaction of the requirements
for the degree of

MASTER OF SCIENCE

in Chemical and Biochemical Engineering

by

Bharath Jagadish

Thesis Committee:
Professor Elizabeth Read, Chair
Professor Hung Nguyen
Professor Nancy Da Silva

2015

TABLE OF CONTENTS

LIST OF FIGURES

LIST OF TABLES

LIST OF ABBREVIATIONS

CD	Cluster of differentiation
CFSE	Carboxyfluorescein succinimidyl ester
CTL	Cytotoxic T lymphocyte
HBV	Hepatitis B virus
HCV	Hepatitis C virus
HIV	Human immunodeficiency virus
IL-2	Interleukin 2
LAG3	Lymphocyte activation gene 3
LCMV	Lymphocytic choriomeningitis
PD-1	Programmed cell death 1
PD-L1	Programmed cell death-ligand 1
PirB	Paired immunoglobulin-like receptor B
TIM3	T-cell immunoglobulin mucin 3

ACKNOWLEDGEMENTS

I would like to thank my thesis advisor, Professor Elizabeth Read, for her constant support, guidance, patience, and encouragement during my years of study here. I would like to thank Professor Hung Nguyen and Professor Nancy Da Silva for serving on my thesis committee.

I would also like to thank my lab mates Brian, Maggie and Benson for their friendship and collaboration. Work would not have been as enjoyable otherwise.

I am deeply grateful to my family and friends in India, who showed me the possibilities and encouraged me to pursue them.

ABSTRACT OF THE THESIS

Mathematical modeling of T-cell exhaustion and PD-1 blockade in chronic infections

By

Bharath Jagadish

University of California, Irvine, 2015

Department of Chemical and Biochemical Engineering

Professor Elizabeth Read, Chair

Immune responses to persistent viral infections often fail because of intense regulation of antigen-specific T-cells–a process referred to as T cell exhaustion, characterized by progressive impairment of cytokine expression, cytotoxicity, and proliferative potential. Reinvigorating exhausted T-cells is considered a promising immunotherapeutic approach to combating chronic viral infections. The inhibitory receptor programmed death 1 (PD-1), is remarkably up-regulated on the surface of exhausted virus-specific CD8+ T-cells. Blockade of this pathway using antibodies against the PD ligand 1 (PD-L1) restores CD8+ T-cell function and reduces viral load. However, the mechanisms that underlie the induction of exhaustion are not completely understood. To investigate the role of PD-1 signaling in chronic viral infections, we have developed a simple mathematical model, formulated as a system of ordinary differential equations, to dissect the dynamics of virus-infected cells, CD8+ T-cells and PD-1 signaling. We estimate rate parameter regimes by fitting to published experiments on mice chronically infected by LCMV. Blockade experiments are performed *in silico* by abruptly reducing PD-1 signaling during the chronic phase of infection. Our

simulations replicate experimental results, showing an increase in frequency and effector function of CD8+ T-cells and decreased viral load upon PD-1 blockade. We use our mathematical model to analyze published measurements of single- and combination-blockade therapy of chronically infected mice. Our analysis shows that anti-LAG3 and anti-TIM3 modulate CD8+ T-cells activity by different mechanisms. Our analysis furthermore shows that the combination blockade by anti-TIM3 and anti-PDL1 results in a synergistic decrease of viral load, whereas the anti-LAG3/anti-PDL1 combination does not.

Chapter 1

Introduction

Virus-specific CD8+ T cells become unresponsive to viral antigens during chronic infection. They persist in a non-functional exhausted state [1] characterized by the inability to produce immune-stimulatory cytokines, lyse virally infected cells and proliferate. Ever since CD8+ T cell exhaustion was characterized in the murine LCMV, such a functional impairment has been observed to be a common feature in human chronic viral infections such as, HIV, hepatitis B virus, hepatitis C virus [2]. These functional defects serve to limit the effectiveness of antigen-specific responses over time and are considered to be one reason for failure of immunological control of the persisting infections.

Recent studies have gained interest in reversing T-cell exhaustion by focusing on the crucial role of inhibitory receptors in regulating T-cell exhaustion during chronic viral infections. The surface inhibitory receptor Programmed death 1 (PD-1) of the CD28 superfamily, was shown to be highly expressed on exhausted CD8+ T cells. Proliferation and function of exhausted T cells can be rescued by blockade of PD-1, which can result in restoration of effective immune responses that control infections and tumors [3-7]. However, expression of other inhibitory receptors like LAG3, TIM3, CTLA4, GP49, 2B4, PirB, and CD160 [8] on exhausted CD8+ T cells indicate that blockade of PD-1 alone may not be sufficient to completely reverse T cell exhaustion.

Inhibitory receptors clearly play a role during chronic infections. But the exact mechanism by which they mediate the T-cell exhaustion is still unknown. PD-1 and CTLA4 are thought to interfere with activation of T-cells, both by reducing co-stimulatory signals at the cell surface through competitive binding to CD80, and by attenuating downstream signaling through TCR or co-stimulatory pathways [9]. An additional mechanism of T cell exhaustion has been described, in which PD-1 signaling actively up-regulates gene expression programs in T cells that are associated with reduced proliferative capacity and effector function [10]. Therefore, the PD-1 pathway appears to mediate exhaustion through multiple mechanisms. Moreover, these mechanisms appear to be to some degree distinct or non-overlapping from those of other receptors.

The complexity of interactions in this type of biological system and the difficulty to isolate influencing factors make the use of mathematics challenging, but valuable. Mathematical models allow us to gain biological insight and improve the interpretation of PD-1 mediated T-cell exhaustion related experimental data. Another advantage of mathematical modeling is that it can be used to unify and interpret data from multiple laboratories and experimental settings. The aim of our research is to provide a comprehensive, predictive and multifaceted approach to quantify the mechanisms responsible for CD8+ T-cell exhaustion. Our main goal is to discover the relative roles played by each immune mechanism during the course of disease and treatment to have a better understanding of what drives the intensity of symptoms, infectivity of the virus and duration of the disease.

Specific objectives were to:

1. Develop a mathematical model of chronic infection that specifically includes PD-1 up-regulation and previously-hypothesized mechanisms of exhaustions.
2. Identify rate parameter ranges most consistent with previous experiments and modeling.
3. Perform *in silico* blockade experiments to determine major mechanisms of PD-1-induced exhaustion alone and in combination with other inhibitory receptors.
4. Determine whether published experimental results support the hypothesis that inhibitory receptors modulate CD8+ T-cell activity in a synergistic manner.

Chapter 2

Background

2.1 Innate and adaptive immune system

An organization of cells and molecules with specialized roles in defending against infection is the immune system [11]. Immune responses fall into two categories - those that occur to the same extent however many times the infectious agent is encountered (innate or natural) and those that improve on repeated exposure to given infection (adaptive or acquired). Innate immune responses range from external barriers (skin, mucous membranes, cilia, secretions) to sophisticated receptors capable of recognizing broad classes of pathogenic organisms. The innate responses use phagocytic cells (neutrophils, monocytes, and macrophages), cells that release inflammatory mediators (basophils, mast cells, and eosinophils), and natural killer cells. The molecular components of innate responses include complement, acute-phase proteins, and cytokines such as the interferons. Adaptive immune responses are mediated by a specialized group of leukocytes, the lymphocytes, which include B cells and T cells. The proliferation of antigen-specific B and T cells occur when the surface receptors of these cells bind to antigen. Specialized cells, called antigen-presenting cells, display the antigen to lymphocytes and collaborate with them in the response to the antigen. B cells secrete immunoglobulins, the antigen-specific antibodies responsible for eliminating extracellular microorganisms. T cells help B cells to make antibody and can also eradicate intracellular pathogens by activating macrophages and by killing virally infected cells. Innate and acquired responses usually work together to eliminate pathogens.

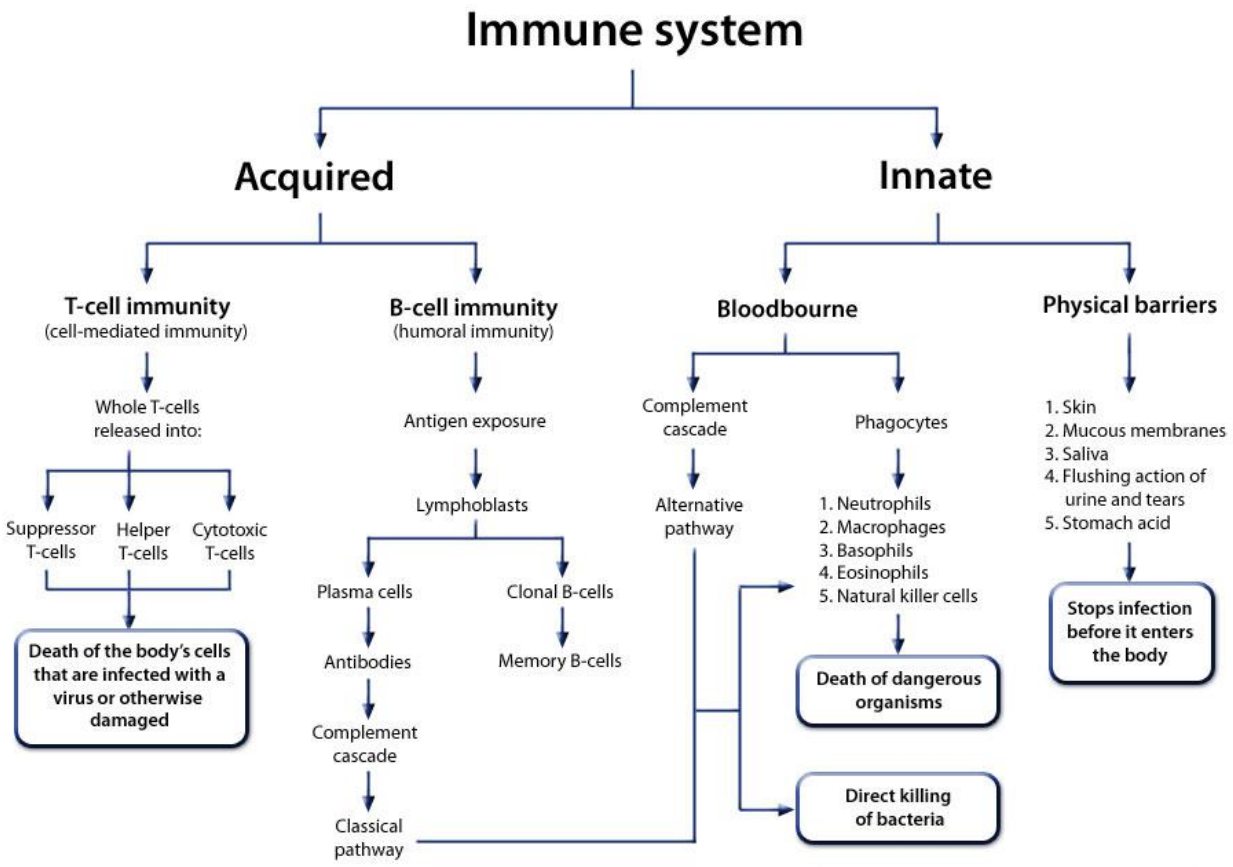

Figure 2.1 Components of the immune system. The principal cells of the immune system and their functions are shown (Elgnainy, 2013).

2.2 T cell activation

Once T cells have completed their development in the thymus, they enter the bloodstream. On reaching a peripheral lymphoid organ, they leave the blood to migrate through the lymphoid tissue, returning via the lymphatics to the bloodstream to recirculate between blood and peripheral lymphoid tissues. Mature recirculating T cells that have not yet encountered their specific antigens are known as naive T-cells. To participate in an adaptive immune response, a naive T-cell must meet its specific antigen, present to it as a

peptide:MHC complex on the surface of an antigen-presenting cell, and be induced to proliferate and differentiate into cells that have acquired new activities that contribute to removing the antigen. These cells are called effector T-cells and, unlike naive T-cells, perform their function as soon as they encounter their specific antigen on other cells. Because of their requirement to recognize peptide antigens presented by MHC molecules, all effector T-cells act on other host cells, not on the pathogen itself. The primary T cell response not only provides effector T-cells but also generates memory T-cells, long-lived cells that give an enhanced response to antigen, which yields protection from subsequent challenge by the same pathogen.

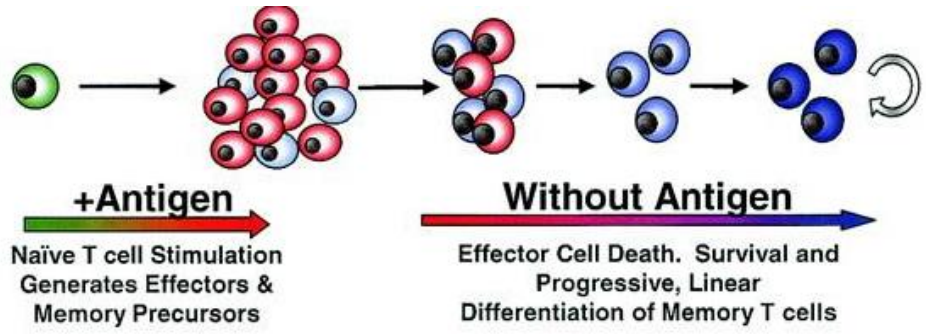

Figure 2.2 Memory CD8 T-cell generation is linear and progressive. Antigenic stimulation causes naïve CD8 T cells to proliferate and acquire effector functions. The effector T cells that survive the death phase further differentiate, giving rise to memory T cells that continue to differentiate in the absence of antigen and acquire the ability to persist in the absence of antigen via homeostatic turnover (Wherry, et al., 2004).

2.3 T-cell exhaustion

An effective CD8+ T-cell response is required to eradicate or control intracellular pathogens. During the acute phase of an infection, antigen-specific CD8+ T cells expand and differentiate into effector cells to clear the pathogens. In the wake of antigen clearance, long-lived memory CD8+ T-cells develop in order to launch an effective secondary response against future infections [13]. Some viruses evade the immune defense and develop into chronic infection. As a consequence, the pool of antigen-specific CD8+ T-cells persist throughout the infection and become dysfunctional. This state of T-cell dysfunction [14] that is characterized by progressive loss of T-cell functions that can culminate in the physical deletion of the responding cells [15] is referred to as CD8+ T-cell exhaustion. The typical loss of functions happens in a hierarchical manner. In the first stage, IL-2 production, high proliferative capacity and ex vivo killing ability are lost. In the intermediate stage, the ability to produce tumor necrosis factor is lost and the final stage of exhaustion is the physical deletion of virus-specific T cells [16-18].

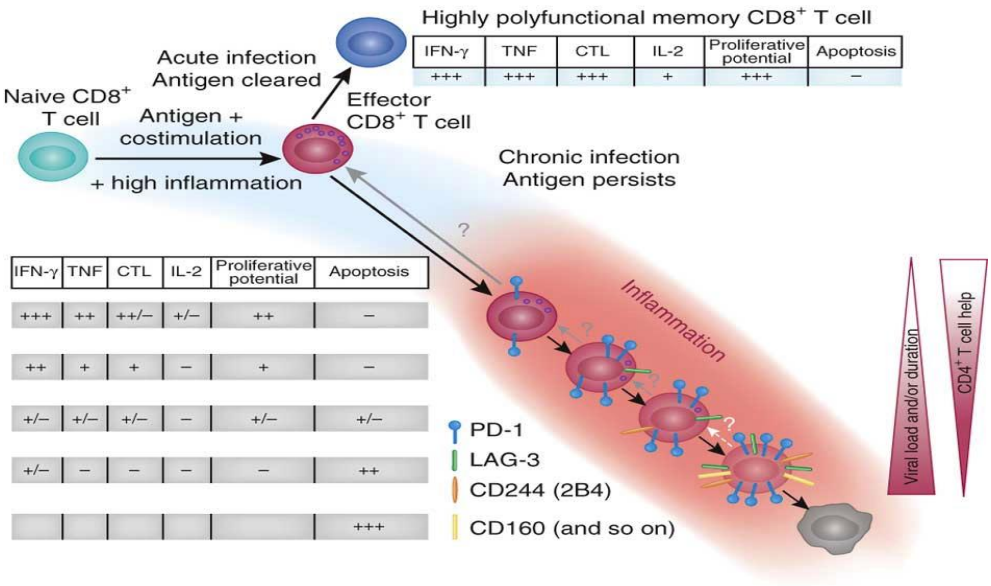

Figure 2.3 Hierarchical T-cell exhaustion during chronic infection (Wherry, 2011)

2.4 Reversing T-cell exhaustion

Studies have indicated that exhausted T-cells are characterized by dramatic up-regulation of multiple inhibitory receptors [2, 19]. During acute infections these receptors function to limit the severity of the response but are then down-regulated as the pathogen is cleared and the memory pool forms [15]. However, during chronic infections, this pattern diverges and establishes an exhausted state that is associated with the constitutive expression of clusters of inhibitory receptors. These receptors collectively operate to negatively regulate the functional and proliferative potential of the responding cells. The identification of the importance of inhibitory receptors in the dysregulation of cellular immune responses in chronically infected hosts has revealed new potential therapeutic targets for restoring immune functions and decreasing viral loads.

Programmed death-1 (PD-1, CD279), a member of the CD28 immunoglobulin super-family of transmembrane proteins expressed as a monomer (PD1, 2) on a wide array of immune cells plays an important role in establishing peripheral tolerance and inhibiting the proliferation and function of T-cells. In LCMV system, PD-1 is markedly upregulated on exhausted T-cells but only transiently expressed on effector T-cells during acute infections, and is not present on the functionally competent memory T-cells. CD8+ T-cells in humans chronically infected with HIV [20-22], HBV [23], and HCV [24] also express high levels of PD-1. Several other receptors have been shown to impair T-cell responses during chronic infections. Cytotoxic T lymphocyte antigen 4 [CTLA-4], which like PD-1 is a CD28 family member, has been shown to impact the functional quality of the T-cell response during HIV-1 and HCV infections of humans [25-27]. T cell immunoglobulin and mucin domain-

containing protein-3 [TIM3] functions to attenuate autoimmune responses and has also been shown to influence the exhausted state. During HIV-1, HCV and LCMV infections, TIM3 is expressed by virus-specific T-cells, and the frequencies and levels of expression parallel the exhausted state of the cells and the severity of infection.

Blocking anti-PD-L1 antibody treatment during chronic LCMV infections promotes the proliferation of virus-specific T-cells, improves their functionality, and reduces viral loads, even in cohorts of CD4-depleted mice, which develop severe T cell exhaustion [3]. As with PD-1, blockade of TIM3 improves the responsiveness and proliferation of the exhausted cells *in vivo*. The hierarchies of inhibitory receptor expression by exhausted cells have been documented during chronic LCMV infection, and these populations of CD8+ T-cells can be segregated into a series of discrete subsets that express different numbers and combinations of inhibitory receptors [8, 28]. More severely exhausted cells express a greater number of inhibitory receptors. The roles of each individual receptor in promoting and sustaining exhaustion are less clear. The inhibitory molecule lymphocyte-activated gene-3 (LAG-3) is widely expressed on exhausted LCMV-specific CD8+ T-cells [28, 29]. Nevertheless, LAG-3 blockade alone is less effective at reversing exhaustion and lowering viral levels than a combined PD-L1 and LAG-3 blocking approach. Therefore, deciphering how specific inhibitory receptor signals integrate to promote and maintain exhaustion will be important.

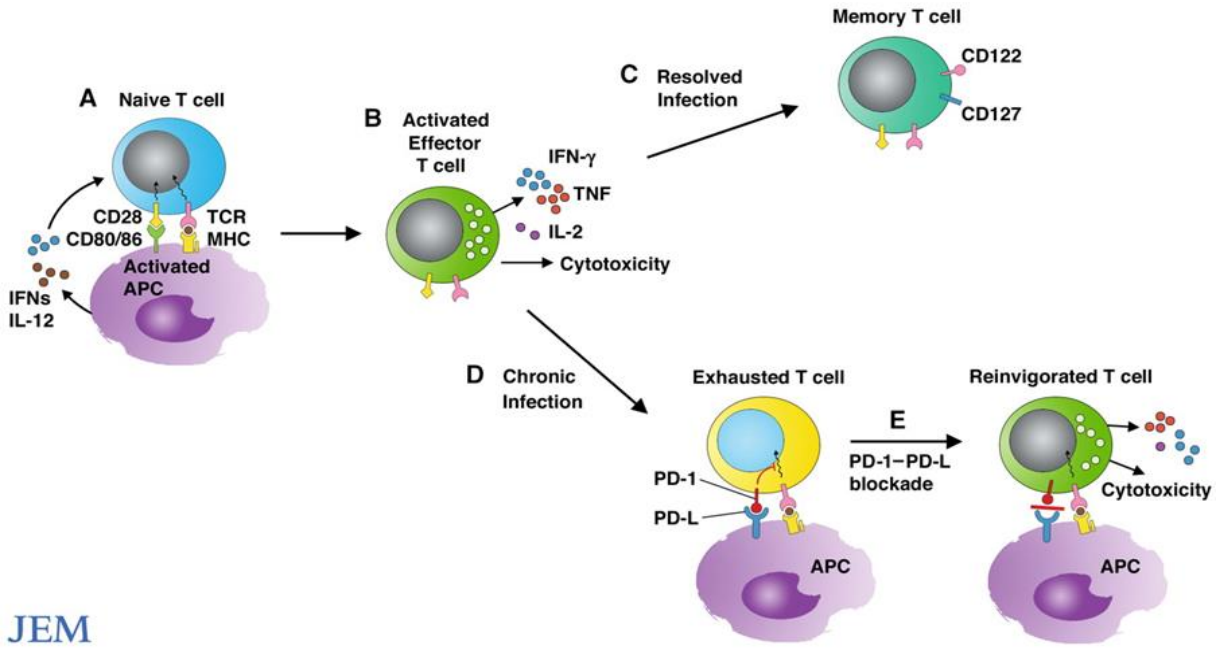

Figure 2.4 Reinvigoration of exhausted T cells by the blockade of interaction of PD-1 with its ligand PD-L1 (Wherry, et al., 2006).

2.5 Mathematical models in immunology

The main objective of this section is to highlight alternative perspectives on the production of various mathematical models of immune processes, and the need for well-founded methodologies for the construction and selection of such a model. We describe some of the contributions that mathematical models have made to our understanding of various aspects of CD8+ T-cell responses to pathogens after chronic infections.

We review three representative models formulated using different types of equations to describe the dynamics of cell populations labeled with CFSE: a heterogeneous ordinary differential equation (ODE) model, a delay differential equation (DDE) model and an age-structured hyperbolic partial differential equation (PDE) model [31].

a. We first consider an ODE based model. A general linear compartmental model considered in [32] describes the rate of changes in the numbers of lymphocytes $N_j(t)$ having undergone j divisions and D(t) the number of dead but not disintegrated lymphocytes at time t. The model assumes that the rates of cell proliferation and death, α_j and β_j, respectively, are division number dependent. In generic form, the model equations are as follows:

$$\frac{dN_j}{dt} = -(\alpha_0 + \beta_0)N_0(t),$$

$$\frac{dN_j}{dt} = 2\alpha_{j-1} N_{j-1}(t) - (\alpha_j + \beta_j)N_j(t), \quad j = 1,\ldots,7$$

$$\frac{dD(t)}{dt} = \sum_{k=0}^{7} \beta_j N_k(t) - \delta D(t)$$

The birth rate and death rate parameters were estimated using the *in vitro* data on the growth of CFSE labeled T-cells. It appeared that the birth rate as a function of the divisions number is bell-shaped, whereas the death rate function is initially zero and increases thereafter.

b. We now consider a model incorporating memory. A well-known biological model for cell cycle data analysis is the Smith-Martin (SM) model, which lumps the cell cycle into two states. The first state (called A) corresponds to G1 phase of the cycle, and the second one (state B) represents S-G2-M phases of the cell cycle. The progression through the cell cycle is assumed to have a stochastic component (the recruitment of cells from an A state into B) and a deterministic component (a progression with a fixed time-lag through the B state). In a recent study a DDE-type model was proposed which describes the rate of change of the population of T lymphocytes in the A and B states that have undergone j divisions:

$$\frac{dA_0}{dt} = -(\alpha_0 + \beta_0)A_0(t),$$

$$\frac{dA_1}{dt} = 2\alpha_0 A_0(t-\tau_0)\exp(-\beta_j \tau_0) - (\alpha + \beta_A)A_1(t),$$

$$\frac{dA_j}{dt} = 2\alpha A_{j-1}(t-\tau)\exp(-\beta B_0) - (\alpha + \beta_A)A_j(t), \qquad j=1,\ldots,\inf$$

$$B_0(t) = \alpha_0 \int_0^{\tau_0} A_0(t-s)\exp(-\beta B_s)\, ds, \; B_j(t) = \alpha \int_0^{\tau} A_j(t-s)\exp(-\beta B_s)\, ds, \qquad j = 1,\ldots., \inf.$$

The parameters of the model characterize separately the division rates and the time-lags of transit through the B state of naive and divided cells as well as the death rates of cells in the A and B states. The range for the division number j was taken to be infinite in order to derive an analytical solution of the models for some special choice of the initial/boundary conditions. In the model variables $A_j(t_i) + B_j(t_i)$ were fitted to *in vivo* data on T lymphocyte distributions with respect to the division number.

c. A model based on PDEs which considers the (with respect to the progression through the B state of the cell cycle) age-structured description of lymphocyte division was analyzed in [32]. For data fitting, the authors considered the population of cells that have undergone j divisions in the A state and in the B state, the latter being defined using the time distribution of cells at time t in the B state $b_j(t, s)$: $B_j(t) = \int_0^{\tau} bj\ (t, s)\ ds$. The corresponding equations read

$$\frac{dA_0}{dt} = 2\alpha b_{j-1}(t, \tau) - (\alpha + \beta_A)A_j(t)$$

$$\frac{db_j(t,s)}{dt} + \frac{db_j}{ds} = -\beta B b_j(t, s), \qquad j = 1, \ldots., \inf$$

To estimate the parameters of the PDE version of the SM model three different parameter estimation approaches (direct fitting, indirect fitting and rescaling method) were examined

[32]. The model proved to be consistent with the *in vivo* data characterizing the CFSE profile of transgenic T-lymphocyte adoptively transferred into irradiated mice. The issue of choosing the right initial conditions for the PDE description received special attention.

The models formulated with general non-linear ODEs represent the dominating class of equations in use in mathematical immunology as they are easy to simulate *in silico* and simpler to analyze qualitatively than many other types of model [30]. The complex short- and long-term dynamics can be portrayed in simple constant coefficient homogeneous equations.

Chapter 3

Mathematical model

3.1 Model development

The model presented here is developed from the work of Johnson et al., [33], which modeled the infection dynamics along with the effects of CD8+ T-cell exhaustion with a series of nonlinear ODEs in mice chronically infected by LCMV. Their model captured the interplay between uninfected target cells (U), virus-infected target cells (V), CD8+ T-cells (X) and the level of exhaustion (Q).

$$\frac{dU}{dt} = a - \beta UV - bU \quad (3.1a)$$

$$\frac{dV}{dt} = \beta UV - (b + \alpha)V - kVX \quad (3.2a)$$

$$\frac{dX}{dt} = sX\frac{V}{(\phi + V)} - \delta X\frac{Q^n}{(q^n + Q^n)} \quad (3.3a)$$

$$\frac{dQ}{dt} = \frac{V}{(\phi + V)} - dQ \quad (3.4a)$$

Table 3.1a A summary of variables used in the model (equations 3.1a -3.4a)

Variable	Description	Initial value
U	Uninfected target cells	1e6
V	Virus infected target cells	1
X	CD8+ T-cells	10
Q	Level of exhaustion	0

Table 3.1b A summary of parameters used in the model (equations 3.1a - 3.4a)

Parameter	Description	Value	Units
a	Rate of production of host cells	1e4	target cells/day
β	Rate of infection	5e-6	$[(\text{target cells})^2.\text{day}]^{-1}$
b	Death rate of host cells	1e-2	$(\text{target cells.day})^{-1}$
α	Rate at which virus infected cells die due to infection	5e-2	$(\text{target cells.day})^{-1}$
k	Rate of clearance of infected cells by the antigen-specific CD8+ T cells	1e-5	$(\text{target cells.T cells. day})^{-1}$
s	Maximum growth rate of CD8+ T cells	1.3	$(\text{T cells.day})^{-1}$
δ	Death rate of CD8+ T cells due to exhaustion	3	$(\text{T cells.day})^{-1}$
ϕ	Antigen density	1e3	target cells
q	Exhaustion threshold	5 - 10	-
d	Rate at which the immune response recovers from exhaustion.	0.1	-

We modify the above Johnson et al. model in such a way that cytotoxic killing of virus infected cells, antigen-dependent growth of CD8+ T-cells and death of CD8+ T-cells are made to be dependent on the level of exhaustion Q, which we will refer to as PD-1 signaling. We assume that CD8+ T cells also proliferate without encountering antigen, and die without undergoing exhaustion. So, our new model is as follows:

$$\frac{dU}{dt} = a - \beta UV - bU \quad (3.1b)$$

$$\frac{dV}{dt} = \beta UV - (b + \alpha)V - k(Q)VX \quad (3.2b)$$

$$\frac{dX}{dt} = s(Q)X\frac{V}{(\phi + V)} + P(Q)X - \delta^{E}(Q)X - \delta X \quad (3.3b)$$

$$\frac{dQ}{dt} = r\frac{V}{(\phi + V)} - dQ \quad (3.4b)$$

where P(Q) is the antigen independent proliferation rate of CD8+ T-cells, $\delta^{E}(Q)$ and δ are PD-1 signaling dependent and independent death rates of CD8+ T-cells respectively.

We introduce a new parameter r, called "blockade parameter", whose reduction is assumed to simulate the blockade of interaction between PD-1 and its ligand PD-L1.

We simplify the model by eliminating the differential equation for U, as the rate of production of host cells differ in each tissue [34]. Now, our exhaustion model is a simplified model of population-dynamics type focusing on the specific effects of PD-1 signaling and blockade on CD8+ T-cell effector function. Our goal is to understand the mechanisms behind T-cell exhaustion.

We describe the system as three coupled differential equations, where each equation gives the rate of change of the particular variable in terms of growth and death, cell-cell kill, and cell inactivation due to PD-1 signaling.

$$\frac{dV}{dt} = pV\left(1-\frac{V}{C}\right) - k(Q)VX \quad (3.1c)$$

$$\frac{dX}{dt} = s(Q)X\frac{V}{(\phi+V)} - \delta(Q)X \quad (3.2c)$$

$$\frac{dQ}{dt} = r\frac{V}{(\phi+V)} - dQ \quad (3.3c)$$

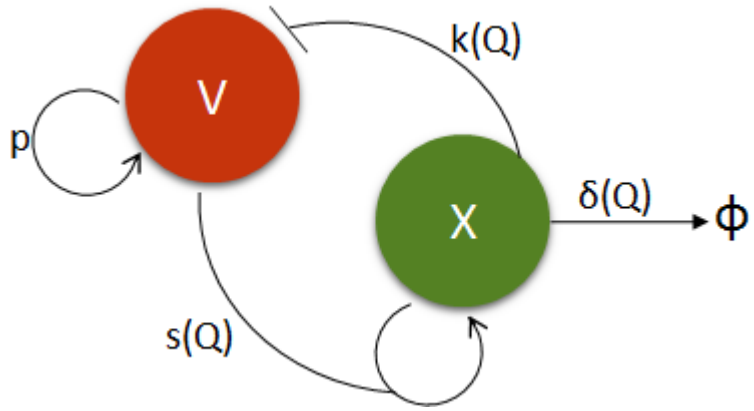

Figure 3.1 Schematic representation of interactions included in the model

Equation (3.1c) of the system describes the rate of change of virus infected cells. It expresses the expansion of virus population at the rate ***p*** from the initial inoculum that can reach a maximum density ***C*** [35], and rate of neutralization of virus infected cells by CD8+ T cells.

Equation (3.2c) characterizes the time rate of change of CD8+ T cells. The proliferation of CD8+ T cells is described by the first term. The rate depends on the density of antigen ***ϕ***. The term ***δ(Q)X*** indicates the loss of functional cells due to exhaustion. CD8+ T-cells are stimulated by the interaction with virus infected cells through a Michaelis-Menten dynamic.

Equation (3.3c) establishes the time rate of change of PD-1 signaling by integrating over the antigenic stimulus and decaying exponentially. We call ***r*** - the blockade parameter; we assume that the reduction of ***r*** simulates the blockade of interaction between PD-1 and its ligand PD-L1. Although our model is similar to that of Johnson et al., if differs in a number of instances that reflect the latest knowledge about mechanisms causing T cell exhaustion. We make the killing rate of CD8+ T cells ***k(Q)***, maximum growth rate of CD8+ T cells ***s(Q)***, and the death rate of CD8+ T cells ***δ(Q)*** dependent on PD-1 signaling, which are implemented as Hill function in the following manner:

$$k(Q) = k^0 \frac{Q^n}{(q_k{}^n + Q^n)}$$

$$s(Q) = s^0 \left(1 - \frac{Q^n}{(q_s{}^n + Q^n)}\right)$$

$$\delta(Q) = \delta^0 \frac{Q^n}{(q_\delta{}^n + Q^n)}$$

where q_k, q_s and q_δ are half-maximal constants and n is the coefficient.

3.2 Simulation

The time course of variables were obtained by numerical integration in MATLAB using ode45, which implements a Runge-Kutta method with a variable time step for efficient computation. We use the dynamical systems analysis software COPASI to estimate the parameters for the model by fitting the model to the experimental data (Blackburn et al.) by adopting evolutionary programming optimization method. We specified the time course data set for viral infected cells and CD8+ T-cells from Blackburn et al. and a finite range of parameter values in COPASI.

Chapter 4

Results and discussion

4.1 Kinetics in chronic infection: Time course simulation of virus infected cells and CD8+ T-cells

We examined whether the simple mathematical models presented above could capture the measured kinetics of viral load and cytotoxic CD8+ T-lymphocytes (CTLs). By fitting the parameter values of the mathematical model, we were able to achieve a good fit to the experimental kinetic data of Blackburn, et al., and the parameter values we found are close in magnitude to those of Johnson, et al. We simulated the dynamics of virus infected cells and CD8+ T-cells by fitting our model defined by the system of ODEs 3.1(b), 3.2 (b), 3.3 (b), 3.4 (b) to Blackburn, et al. experimental data and estimated rate parameters shown in Table 4.1.

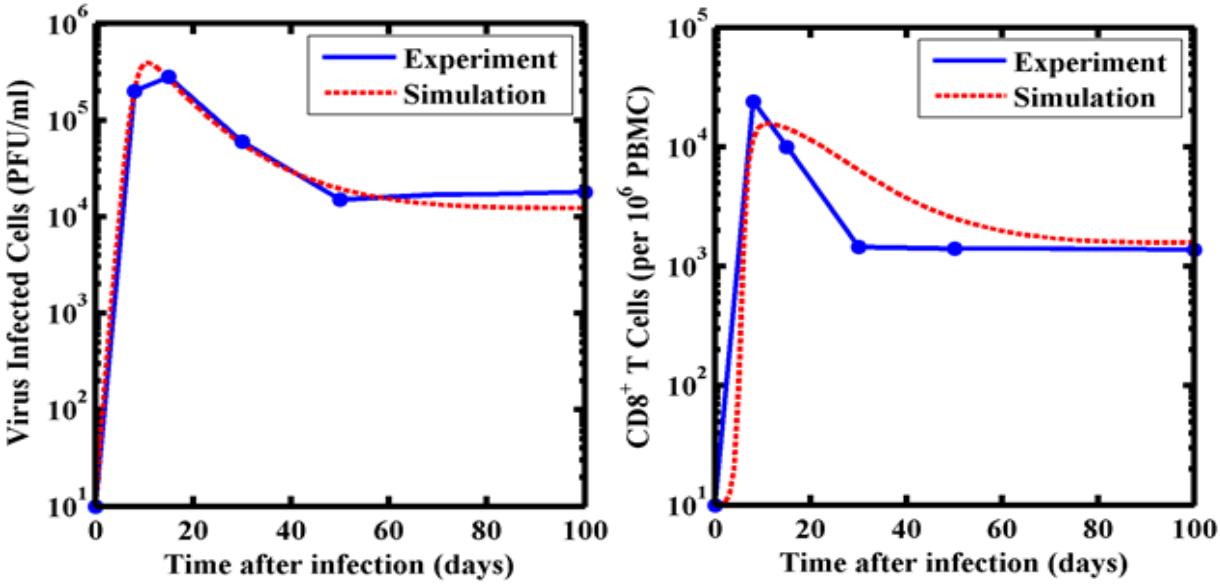

Figure 4.1 The model described by equations 3.1(b) – 3.4(b) is fit to the LCMV data of Blackburn et al.

Table 4.1 Parameter estimates obtained from COPASI (equations 3.1b - 3.4b)

Parameter	Description	Value	Units
a	Rate of production of host cells	.7e4	target cells/day
β	Rate of infection	5e-6	$[(\text{target cells})^2.\text{day}]^{-1}$
b	Death rate of host cells	5e-2	$(\text{target cells.day})^{-1}$
α	Rate at which virus infected cells die due to infection	5e-2	$(\text{target cells.day})^{-1}$
k	Rate of clearance of infected cells by the antigen-specific CD8+ T cells	3.5e-5	$(\text{target cells.T cells. day})^{-1}$
s	Maximum growth rate of CD8+ T cells	1.2	$(\text{T cells.day})^{-1}$
δ	Death rate of CD8+ T cells due to exhaustion	1.1	$(\text{T cells.day})^{-1}$
ϕ	Antigen density	1.25e4	target cells
d	Rate at which the immune response recovers from exhaustion.	0.1	-
q_k	Half maximal-constants	2.3e6	-
q_s		1.04e4	-
q_P		1.9	-
q_δ		3.36e3	-

4.2 *In vivo* blockade of PD-1

We utilized the data for single- and combination-blockade therapy of mice infected with chronic (clone 13) LCMV from Blackburn, et al., [28] and Jin, et al [36]. In both studies, drug treatment was begun on day 28 post-infection, and measurements of viral loads and CTL responses were performed two weeks later (day 42). A consistent feature of the experimental data in both studies is that the increase of CD8+ T cells after blockade therapy appears to be correlated with the decrease of viral load after therapy in infected tissues. We analyzed the data using our mathematical model, to determine how this correlation depended on the type of therapy (anti-PD-L1, alone or in combination with anti-LAG3 or anti-TIM3) and type of infected tissue.

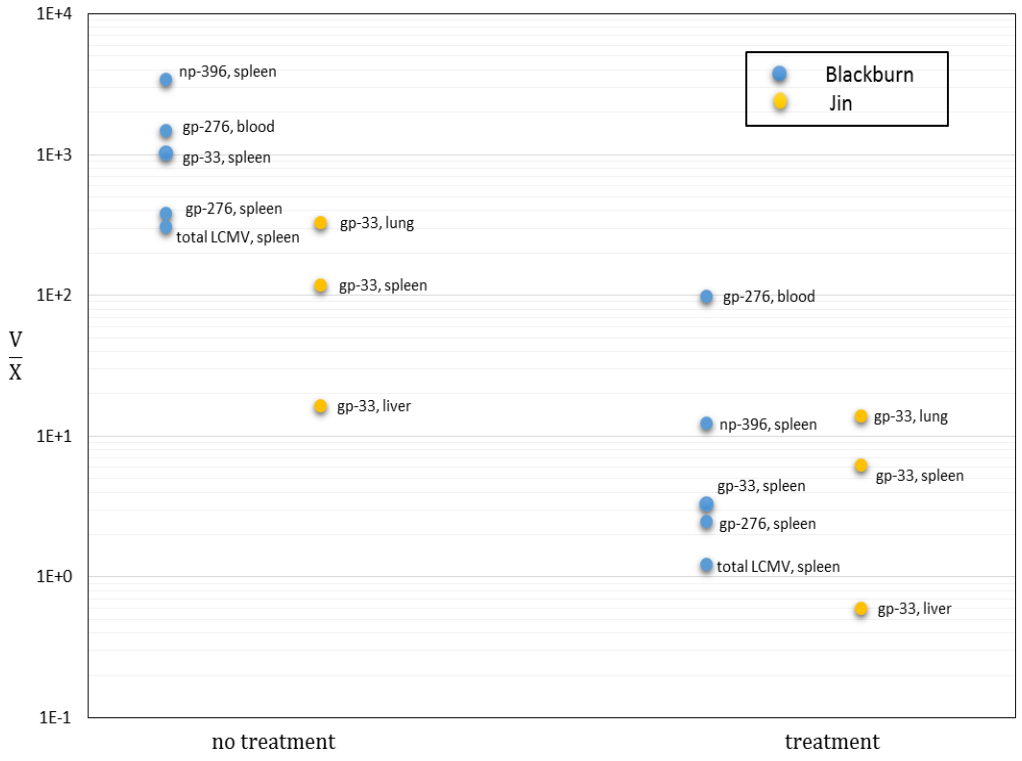

Figure 4.2 Ratio of total number of virus infected cells to CD8+ T cells on day 28 and on day 42 in response to α-PD-L1 therapy.

4.3 *In silico* blockade simulation

We assessed the role of inhibitory receptor PD-1 on exhausted CD8+ T cells *in silico* by reducing the "blockade parameter"-***r*** on day 28 of the infection. Blockade of PD-1 reproduced the key qualitative effects seen in Blackburn, et al and Jin, et al. There was a decrease in number of viral infected cells and increase in the CD8+ T cells after blockade

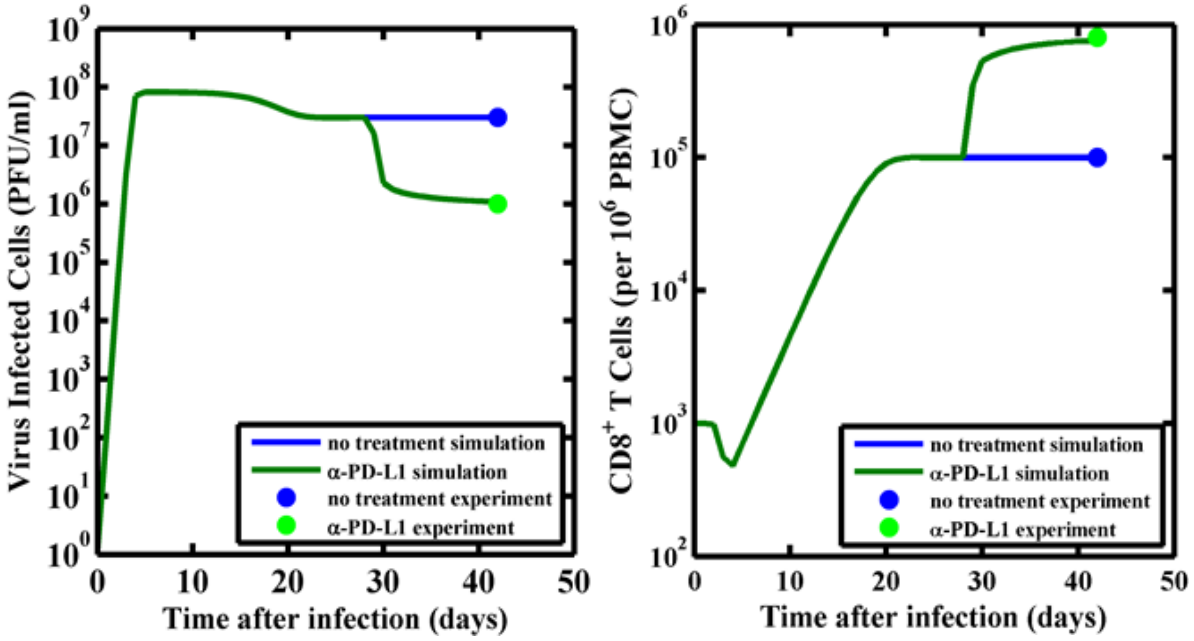

Figure 4.3a Dynamics of V and X according to the modified model (equations 3.1(c) - 3.3 (c)) with the steady state data points on day 42 of treatment for spleen (Blackburn, et al. [28]). Treatment begins on day 28, and the effect of PD-1 blockade is clearly visible with the decrease in V and increase in X as time progressed and ultimately reached steady state.

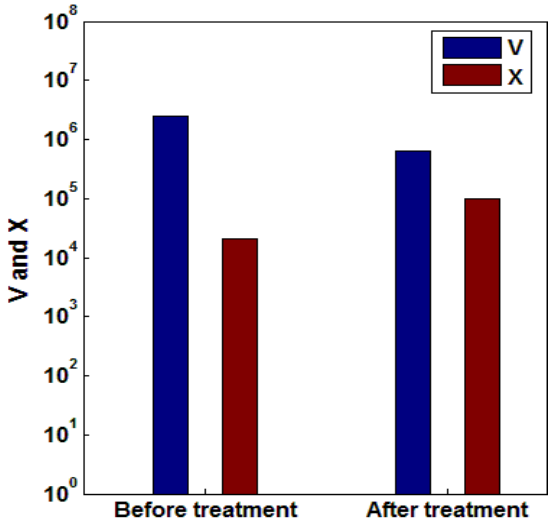

Figure 4.3b V and X from the above simulation on day 28 (before α-PD-L1 treatment) and day 42 (after α-PD-L1treatment).

4.4 Steady state analysis

We performed a steady state and stability analysis for the model 3.1–3.3(c). The system has 3 steady states:

- (V, X, Q) = (0, 0, 0) (4.1)
- (V, X, Q) = $\left(0, 0, \frac{Cr}{d(C+\phi)}\right)$ (4.2)
- (V, X, Q) = $\left(\frac{-\delta(Q)\phi}{\delta(Q)-s(Q)}, \frac{p}{k(Q)}\left[1+\frac{\delta(Q)\phi}{C(\delta(Q)-s(Q))}\right], \frac{\delta(Q)r}{ds(Q)}\right)$ (4.3)

It is possible to determine the stability of our system by the sign of real part of eigenvalues of the Jacobian matrix. The Jacobian matrix of our system of ODEs is the matrix of the partial derivatives of the right-hand side with respect to state variables.

$$\text{Jacobian} = \begin{bmatrix} -Xk(Q) + p\left(1 - \frac{Vp}{C}\right) & -Vk(Q) & VXk(Q)k^{0^2}(k(Q)-1) \\ \frac{Xs(Q)}{V+phi} - \frac{VXs(Q)}{(V+phi)^2} & \frac{Vs(Q)}{V+phi} - \delta(Q) & -VX\frac{Q}{Q+q_s}s(Q) - X\delta^0\frac{Q}{q_\delta+1} \\ \frac{r}{V+phi} - \frac{Vr}{(V+phi)^2} & 0 & -d \end{bmatrix}$$

We substitute the three steady state solutions for V, X and Q and estimate the following eigenvalues.

$$e_1 = \begin{Bmatrix} p \\ -d \\ -\delta \end{Bmatrix}$$

$$e_2 = \begin{Bmatrix} -d \\ -p \\ -\left(\frac{C(\delta - s) + \delta\phi}{C + \phi}\right) \end{Bmatrix}$$

$$e_3 = \begin{Bmatrix} -d \\ \dfrac{-(\delta ps\{4C^2(\delta^3 - s^3) + 12C^2\delta s(s - \delta) + \ldots \\ \qquad 4C\delta\phi(\delta^2 - 2s + s^2) + p\delta\phi^2 s\})^{1/2} + \delta p\phi s}{2Cs(\delta - s)} \\ \dfrac{(\delta ps\{4C^2(\delta^3 - s^3) + 12C^2\delta s(s - \delta) + \ldots \\ \qquad 4C\delta\phi(\delta^2 - 2s + s^2) + p\delta\phi^2 s\})^{1/2} - \delta p\phi s}{2Cs(\delta - s)} \end{Bmatrix}$$

where e_1, e_2 and e_3 are the eigenvalues corresponding to steady state solutions (4.1), (4.2) and (4.3) respectively and s = s(Q) and δ = δ(Q)

We plug in the following parameter values to determine the numerical values of eigenvalues.

C = 5e5, p = 5, ϕ(Q) = 1.67e5, δ(Q) = 1.2, s(Q)= 2, d = 10

Now, $e_1 = \begin{bmatrix} -10 \\ 1.2 \\ 5 \end{bmatrix}$, $e_2 = \begin{bmatrix} -10 \\ -5 \\ 0.3 \end{bmatrix}$, $e_3 = \begin{bmatrix} -10 \\ -1.85 \\ -0.65 \end{bmatrix}$

As all the eigenvalues in e_3 have negative real parts, (4.3) provides a stable steady state solution.

Solution (4.1) is not of interest, because all species are 0. Solution (4.2) represents a steady-state viral load that reaches capacity, in the absence of any immune response. Solution (4.3) corresponds to a steady-state equilibrium between the virus and the CTL response. In previous mathematical modeling studies, such an equilibrium state has been identified as representing a chronic infection scenario, where a non-zero CTL response maintains the virus in steady-state, but does not successfully clear the virus. So, solution (3) provides stable steady state values for the model, and the model is capable of capturing the stable equilibrium between virus and the CTL response that is seen in chronic viral infections.

4.5 Sensitivity analysis to examine qualitative effects of blockade treatment:

We investigated the sensitivity of model variables by studying the effect of changes in the parameters that depend on PD-1 signaling. It is possible to examine the robustness of infection dynamics to parameter values and to explore to which parameters the system is more sensitive to understand key immune system mechanisms.

Table 4.2 One-dimensional sensitivity analysis on model parameters.

Parameter	Range	Model behavior
s	1 - 5	There is a dramatic decrease in viral infected cells with increase in s. However, CD8+ T-cells increase and reach a steady state with increase in s.
δ	0 - 2	The higher δ, the higher the damage to the susceptible tissue as CD8+ T-cells go down to zero.
k	10^{-8} - 1	Changes in k has no effect on virus infected cells. But CD8+ T cells decrease sharply with slight increase in k.

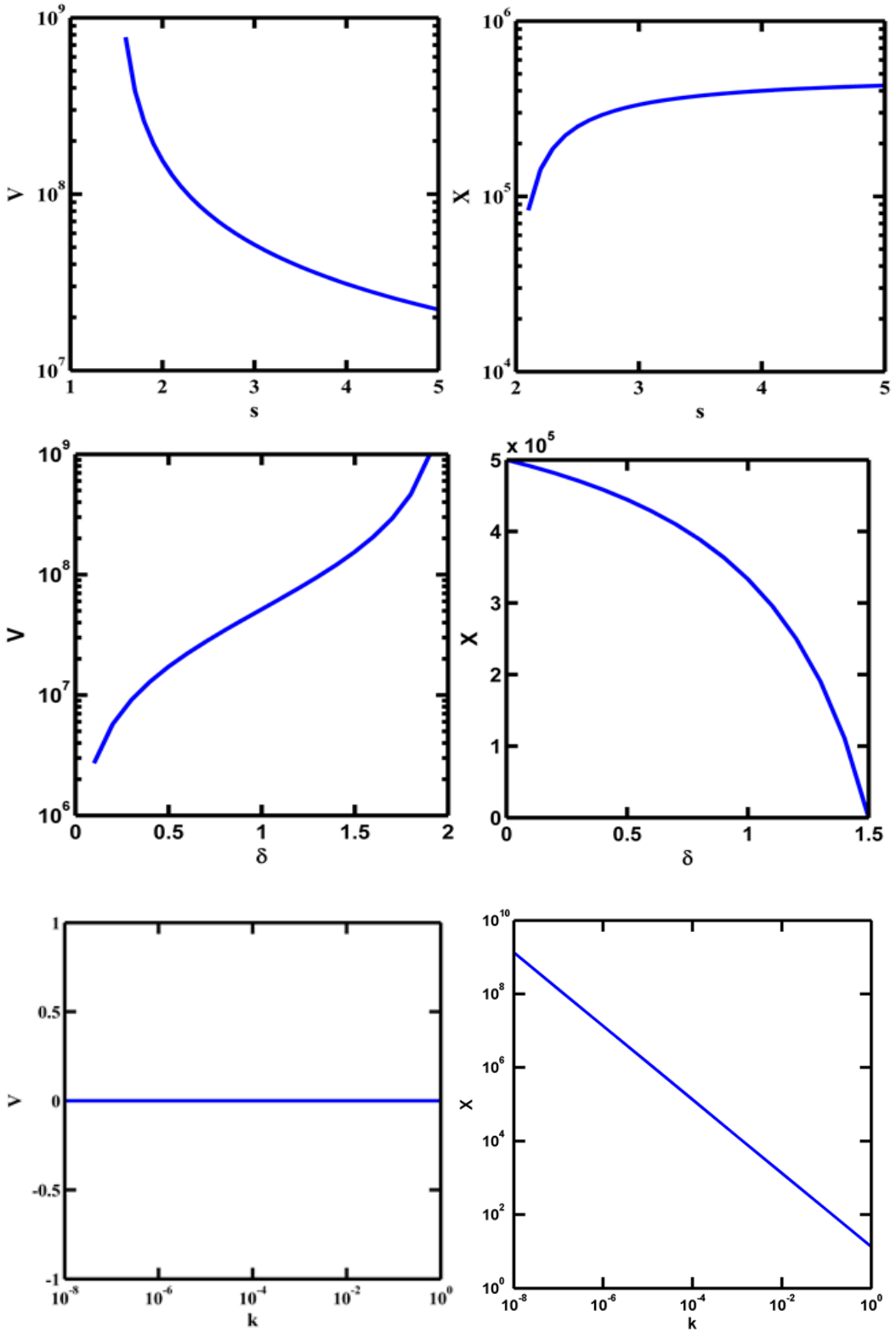

Figure 4.4 One-dimensional sensitivity analyses. Steady state values of V and X vs parameters

Figure 4.4 shows that blockade treatment could work by different mechanisms. If treatment increases the proliferation rate of CTLs (parameter *s*), that would result in a decreased viral load and increased CTLs, which qualitatively agrees with the trend seen in the data from Blackburn, et al., and Jin, et al. Similarly, if blockade treatment decreases the CTL apoptosis rate (parameter δ), that would also have the correct qualitative effect. However, if blockade treatment modulates only parameter k (the rate of infected cell killing by CTLs), that would not have the appropriate effect, because the viral load would be unchanged. Therefore, blockade treatment must have an effect on either *s* or δ (or both) in order to recapitulate the trend observed in experiments.

4.6 Analysis of per-cell killing efficiency

If we assume that the system has reached steady-state by day 42 after treatment, then we can calculate the per-cell killing efficiency of CTLs based on the measured values of viral infected cells and T cells. This allows us to determine whether the killing efficiency is affected by the blockade treatment.

At steady state,

$\frac{dV}{dt} = 0 = pV\left(1 - \frac{V}{C}\right) - kVX$

So, $k = \frac{P}{X}\left(1 - \frac{V}{C}\right)$

If we used the value of $p = 5$ day^{-1} assumed by Ganusov, et al., [35] we can directly calculate k for different values of C, the carrying capacity of virus for a particular tissue.

Figure 4.5 shows the calculated ratio of $\frac{k^t}{k^u}$, that is the per-cell killing efficiency after treatment to before treatment, respectively. By analyzing the data in Blackburn, et al., [28]

we find that for most parameter values, the per-cell killing efficiency is higher after anti-LAG3 treatment, but lower after anti-PD-L1 combination therapy. In analysis of the Jin, et al., [36] data we find that both anti-TIM3 and anti-PD-L1 decrease the per-cell killing efficiency. Both studies show the same qualitative effect, which is that anti-PD-L1 has the stronger effect of the single-drug therapies, while the combination therapy shows the greatest effect.

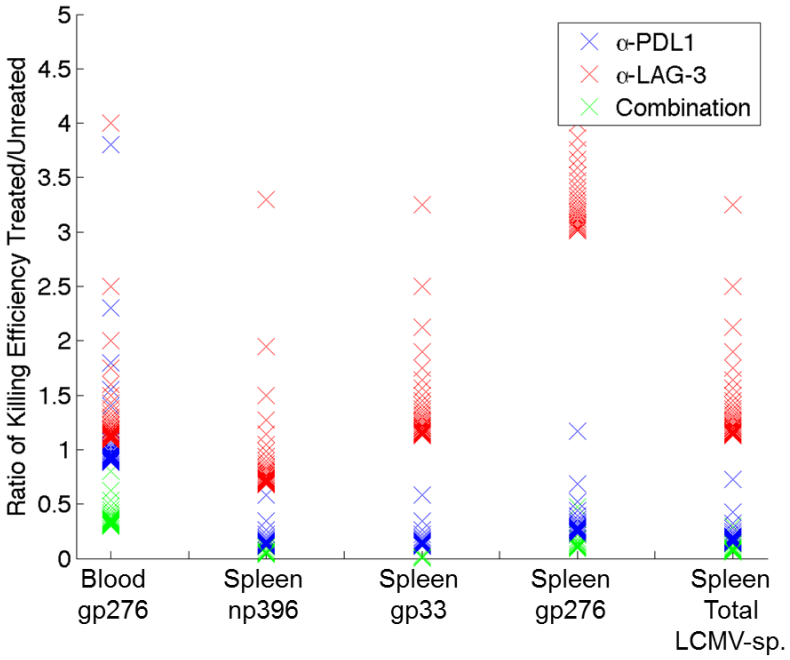

Figure 4.5a Inference of per-cell killing efficiencies from Blackburn, et al. [28] Values plotted are calculated based on the data from Blackburn, et al. [28] and the mathematical model. For each tissue, specificity, and drug-type, $\frac{k^t}{k^u}$ is calculated for a range of values of the unknown parameter C (the viral load carrying capacity). For most values of C, the anti-LAG-3 treatment results in an increased per-cell killing efficiency ($\frac{k^t}{k^u}$>1), while for anti-PD-L1 and combination therapy, the per-cell killing efficiency is decreased ($\frac{k^t}{k^u}$<1).

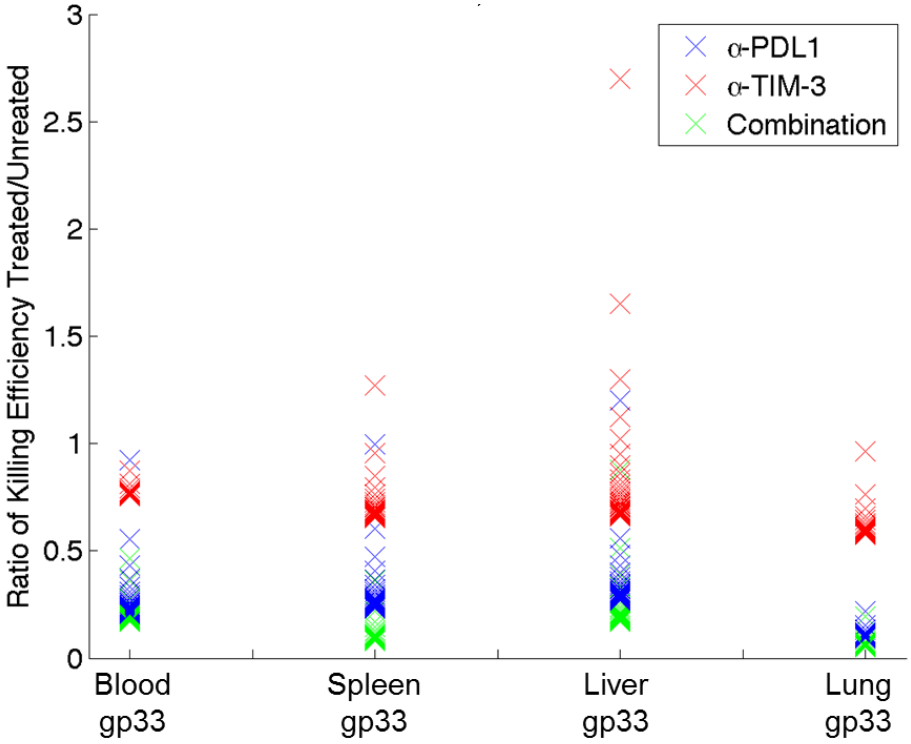

Figure 4.5b Inference of per-cell killing efficiencies from Jin, et al. [36] The data from Jin, et al., show qualitative similarity to those of Blackburn, et al. [28] Per-cell killing efficiencies are decreased most upon combination therapy. Anti-Tim3 treatment decreases per-cell killing efficiencies for most values of C, but not as much as anti-PD-L1 therapy alone or in combination.

4.7 Analysis of proliferation/apoptosis

By a steady-state assumption on X (the CTL response), we can infer the correct value of $\frac{s}{\delta}$ in the model.

At steady state,

$$\frac{dX}{dt} = 0 = s\left(\frac{XV}{\phi+V}\right) - \delta X$$

So, $\frac{s}{\delta} = \frac{\phi+V}{V}$

In the treatment scenarios, we can calculate $\frac{\left(\frac{s}{\delta}\right)^t}{\left(\frac{s}{\delta}\right)^u}$ equivalent to $\frac{(\phi+V^t)V^u}{(\phi+V^u)V^t}$, where Φ is an unknown parameter. The maximum of this expression is given by $\frac{V^u}{V^t}$. Therefore, this ratio gives a measure of how much the net proliferation rate $\left(\frac{s}{\delta}\right)$ is increased after treatment. We see that in both the Blackburn and Jin studies, the combination treatment has the largest effect on the net proliferation rate of CTLs. We can furthermore calculate the ratio of $\frac{V^u}{V^t}$ that would be seen using a Bliss-independence model [37] for the combination therapy. The Bliss-independence model is a commonly-used measure to determine whether two drugs in combination have a greater (i.e., synergistic) or lesser (i.e., antagonistic) effect than would be expected if they functioned independently.

Table 4.3 Fraction of virus infected cells surviving according to single drug, combination and Bliss independence.

	Drug 1	**Drug 2**	**Combination**	**Bliss independence**
Fraction Surviving	$S_1 = \frac{V^t}{V^u}$	$S_2 = \frac{V^t}{V^u}$	S_c	$S_1 \times S_2$

If $S_c < S_1 \times S_2$, the combination treatment is thought to be synergistic; if $S_c > S_1 \times S_2$ the combination treatment is not synergistic

In analysis of the Blackburn data, we see that the combination of anti-PDL1 and anti-LAG3 is not synergistic in all tissues except the kidney. However, in analysis of the Jin data, we see that the combination therapy is synergistic (i.e., exceeding the Bliss-independence criterion) in all tissues.

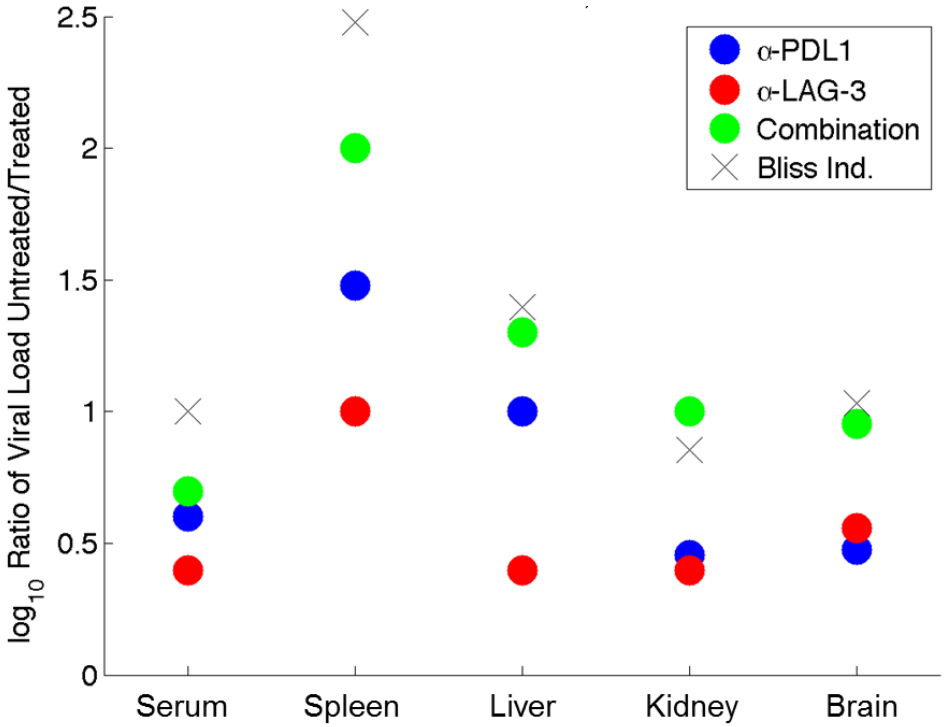

Figure 4.6a Inference of proliferation/apoptosis rates from Blackburn, et al. [28] Plotted values are $\log_{10}\left(\frac{v^u}{v^t}\right)$, where $\frac{v^u}{v^t}$ is related to $\frac{\left(\frac{s}{\delta}\right)^t}{\left(\frac{s}{\delta}\right)^u}$, the ratio of proliferation/apoptosis rates of CTLs after and before treatment. In every case except the kidney, the same qualitative trend is seen, where each drug treatment decreases viral load, with the effect being least significant for the single-drug anti-LAG3 treatment, and most significant for the treatment combinations with anti-PD-L1. These results indicate that the $\frac{s}{\delta}$ ratio of CTLs is highest for combination therapy. However, as compared to the Bliss independence model of synergy (×), the anti-PDL1/anti-LAG-3 combination therapy is not synergistic, except in the case of the kidney.

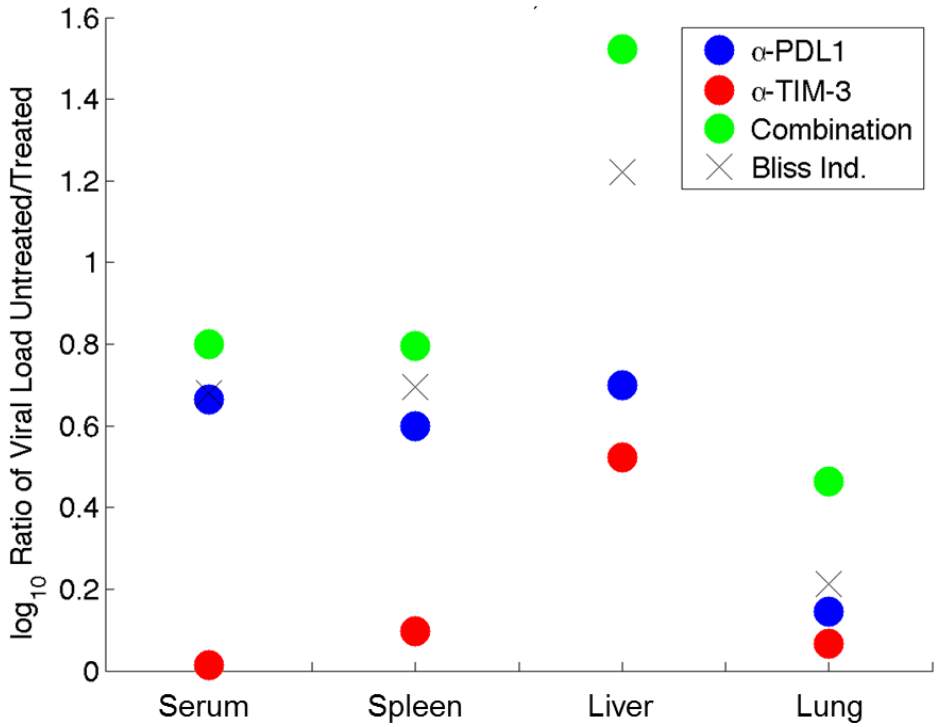

Figure 4.6b Inference of proliferation/apoptosis rates from Jin, et al. As in Blackurn, et al., [28] a similar trend is seen, where the single-drug anti-TIM-3 treatment is least effective at reducing viral load, while the combination treatment with anti-PD-L1 is most effective. As compared to the Bliss-independence model of synergy (×), the anti-PD-L1/anti-TIM3 combination therapy appears synergistic in all 4 tissues measured, as indicated by the $\frac{v^u}{v^t}$ ratio exceeding that of the Bliss independence model in all cases.

Taken together, the above analysis shows that all three drugs (anti-PD-L1, anti-LAG-3, anti-Tim-3) modulate CD8+ T-cells activity by increasing the net proliferation rate (proliferation/apoptosis rates). However, the analysis reveals a mechanistic difference between the function of anti-LAG3 and anti-TIM3: in addition to modulating the net proliferation rate of CD8+ T-cells, anti-LAG3 also functions by increasing the per-CD8+ T-cell killing efficiency (k). While anti-TIM3/anti-PD-L1 showed more synergy, the anti-PD-

L1/anti-LAG3 combination was overall more effective in reducing viral loads, according to the measurements of Blackburn, et al. [28]

Chapter 5

Conclusions and future directions

We developed a simple ODE based mathematical model to investigate the role of PD-1 signaling in chronic viral infections. Our model is in good agreement with the experiment, reproducing the kinetics of virus infected and CD8+ T-cells. We performed blockade experiments *in silico*, the simulations of which reproduced the experimental results, showing a decreased frequency in virus infected cells and increased frequency in CD8+ T cells. We explored the different mechanisms by which the blockade experiments worked by performing steady state and sensitivity analyses. We showed that blockade therapy must have an effect on either proliferation rate or apoptosis rate (or both) of CD8+ T-cells in order to replicate the results of blockade experiments. Our investigations on the effect of single drug and combined drug therapies indicated that anti-PD-L1/anti-TIM3 and anti-LAG3 worked by different mechanisms, as anti-PD-L1/anti-TIM3 decreased per-cell killing efficiencies but anti-LAG3 increased per-cell killing efficiencies. Future studies should analyze alternative models that could provide better insights into the mechanisms of CD8+ T-cells killing. We also showed that anti-TIM3 and anti-PD-L1 behave synergistically, whereas anti-LAG3 and anti-PD-L1 do not. A kinetic model that includes the possibility of synergistic or antagonistic behavior of drugs in combination could be useful in further quantifying the degree of synergy between drugs.

Chapter 6

References

1. Wherry, E. J. & Ahmed, R. Memory CD8 T-cell differentiation during viral infection. *J. Virol.* **78,** 5535–5545 (2004).

2. Shin, H. & Wherry, E. J. CD8 T cell dysfunction during chronic viral infection. *Curr. Opin. Immunol.* **19,** 408–415 (2007).

3. Barber, D. L. *et al.* Restoring function in exhausted CD8 T cells during chronic viral infection. *Nature* **439,** 682–687 (2006).

4. Fourcade, J. *et al.* Upregulation of Tim-3 and PD-1 expression is associated with tumor antigen-specific CD8+ T cell dysfunction in melanoma patients. *J. Exp. Med.* **207,** 2175–2186 (2010).

5. Sakaguchi, S., Yamaguchi, T., Nomura, T. & Ono, M. Regulatory T cells and immune tolerance. *Cell* **133,** 775–787 (2008).

6. Butler, N. S. *et al.* Therapeutic blockade of PD-L1 and LAG-3 rapidly clears established blood-stage Plasmodium infection. *Nat. Immunol.***13,** 188–195 (2012).

7. Topalian, S. L., Drake, C. G. & Pardoll, D. M. Targeting the PD-1/B7-H1 [PD-L1] pathway to activate anti-tumor immunity. *Curr. Opin. Immunol.* **24,** 207–212 (2012).

8. Wherry, E. J. *et al.* Molecular signature of CD8+ T cell exhaustion during chronic viral infection. *Immunity* **27,** 670–684 (2007).

9. Penaloza-MacMaster, P. *et al.* Interplay between regulatory T cells and PD-1 in modulating T cell exhaustion and viral control during chronic LCMV infection. *J Exp Med* **211,** 1905–1918 (2014).

10. Quigley, M. *et al.* Transcriptional analysis of HIV-specific CD8+ T cells shows that PD-1 inhibits T cell function by upregulating BATF. *Nat. Med.* **16,** 1147–1151 (2010).

11. Delves, P. J. & Roitt, I. M. The Immune System. *New England Journal of Medicine* **343,** 37–49 (2000).

12. Elgnainy, H. *Immunology I* ,THE PHYSIOLOGY OF THE IMMUNE SYSTEM | The Amazing Medicine (2013) http://theamazingmedicine.blogspot.com/2013/07/immunology-i-physiology-of-immune-system.html>

13. Buggert, M. *et al.* T-bet and Eomes Are Differentially Linked to the Exhausted Phenotype of CD8+ T Cells in HIV Infection. *PLoS Pathog* **10,** e1004251 (2014).

14. Wherry, E. J. T cell exhaustion. *Nat Immunol* **12,** 492–499 (2011).

15. Yi, J. S., Cox, M. A. & Zajac, A. J. T-cell exhaustion: characteristics, causes and conversion. *Immunology* **129,** 474–481 (2010).

16. Zajac, A. J. *et al.* Viral immune evasion due to persistence of activated T cells without effector function. *J. Exp. Med.* **188,** 2205–2213 (1998).

17. Wherry, E. J., Blattman, J. N., Murali-Krishna, K., van der Most, R. & Ahmed, R. Viral persistence alters CD8 T-cell immunodominance and tissue distribution and results in distinct stages of functional impairment. *J. Virol.* **77,** 4911–4927 (2003).

18. Moskophidis, D., Lechner, F., Pircher, H. & Zinkernagel, R. M. Virus persistence in acutely infected immunocompetent mice by exhaustion of antiviral cytotoxic effector T cells. *Nature* **362,** 758–761 (1993).

19. Shin, H., Blackburn, S. D., Blattman, J. N. & Wherry, E. J. Viral antigen and extensive division maintain virus-specific CD8 T cells during chronic infection. *J Exp Med* **204,** 941–949 (2007).

20. Day, C. L. *et al.* PD-1 expression on HIV-specific T cells is associated with T-cell exhaustion and disease progression. *Nature* **443,** 350–354 (2006).

21. Petrovas, C. *et al.* PD-1 is a regulator of virus-specific CD8+ T cell survival in HIV infection. *J. Exp. Med.* **203,** 2281–2292 (2006).

22. Trautmann, L. *et al.* Upregulation of PD-1 expression on HIV-specific CD8+ T cells leads to reversible immune dysfunction. *Nat Med* **12,** 1198–1202 (2006).

23. Boettler, T. *et al.* Expression of the interleukin-7 receptor alpha chain (CD127) on virus-specific CD8+ T cells identifies functionally and phenotypically defined memory

T cells during acute resolving hepatitis B virus infection. *J. Virol.* **80,** 3532–3540 (2006).

24. Urbani, S. *et al.* PD-1 expression in acute hepatitis C virus (HCV) infection is associated with HCV-specific CD8 exhaustion. *J. Virol.* **80,** 11398–11403 (2006).
25. Kaufmann, D. E. *et al.* Upregulation of CTLA-4 by HIV-specific CD4+ T cells correlates with disease progression and defines a reversible immune dysfunction. *Nat. Immunol.* **8,** 1246–1254 (2007).

26. Nakamoto, N. *et al.* Synergistic Reversal of Intrahepatic HCV-Specific CD8 T Cell Exhaustion by Combined PD-1/CTLA-4 Blockade. *PLoS Pathog* **5,** (2009).

27. Cecchinato, V. *et al.* Immune activation driven by CTLA-4 blockade augments viral replication at mucosal sites in simian immunodeficiency virus infection. *J. Immunol.* **180,** 5439–5447 (2008).

28. Blackburn, S. D. *et al.* Coregulation of CD8+ T cell exhaustion by multiple inhibitory receptors during chronic viral infection. *Nat. Immunol.* **10,** 29–37 (2009).

29. Richter, K., Agnellini, P. & Oxenius, A. On the role of the inhibitory receptor LAG-3 in acute and chronic LCMV infection. *Int. Immunol.* **22,** 13–23 (2010).

30. Freeman, G. J., Wherry, E. J., Ahmed, R. & Sharpe, A. H. Reinvigorating exhausted HIV-specific T cells via PD-1–PD-1 ligand blockade. *J Exp Med* **203,** 2223–2227 (2006).

31. Andrew, S. M., Baker, C. T. H. & Bocharov, G. A. Rival approaches to mathematical modelling in immunology. *Journal of Computational and Applied Mathematics* **205,** 669–686 (2007).

32. Luzyanina, T. *et al.* Computational analysis of CFSE proliferation assay.*J Math Biol* **54,** 57–89 (2007).

33. Johnson, P. L. F. *et al.* Vaccination Alters the Balance between Protective Immunity, Exhaustion, Escape, and Death in Chronic Infections. *J. Virol.* **85,** 5565–5570 (2011).

34. Ganusov, V. V. *et al.* Quantifying cell turnover using CFSE data. *J. Immunol. Methods* **298,** 183–200 (2005).

35. Ganusov, V. V., Barber, D. L. & De Boer, R. J. Killing of Targets by CD8+ T Cells in the Mouse Spleen Follows the Law of Mass Action. *PLoS ONE* **6,** e15959 (2011).

36. Jin, H. T. *et al.* Cooperation of Tim-3 and PD-1 in CD8 T-cell exhaustion during chronic viral infection. *Proc. Natl. Acad. Sci. U.S.A.* **107,** 14733–14738 (2010).

37. Greco, W. R., Bravo, G. & Parsons, J. C. The search for synergy: a critical review from a response surface perspective. *Pharmacol. Rev.***47,** 331–385 (1995).